RESEARCH ARTICLE OPEN ACCESS

Analysis of Modulation Index and Switching Frequency Impact On the Three-Level Neutral Point Clamped Converter Efficiency

Mrs. E. Sreeshobha
Department of Electrical and Electronics Engineering, University College of Engineering, Osmania University, Hyderabad, Telangana, India.

Abstract: Increasing focus on green energy generation and environmental ecology, expanding the solar power generation and hybrid electric vehicles practice. Higher demand for Neutral Point Clamped (NPC) converters in green energy generation and environmental protection areas is the main motivation behind the analysis of NPC converter operation for different modulation Indices and frequencies with which IGBT is turned on and off. Sinusoidal pulse width modulation (SPWM) implemented with the aid of MATLAB Simulink tool for three-phase NPC converter operation. Each switching element's power losses and temperature are simulated with the Fuji IGBT Simulator tool. The Systematic method of NPC converter, total losses evaluation is presented, and obtained losses are validated with analytical losses. The effect of SPWM and modulation index (MI) on the converter losses, is verified. Variation of converter efficiency as a function of modulation index and frequency of turning on and off is obtained and analyzed. The proposed approach and analysis will suggest the relevant operating mode of a converter for a specific application.

Keywords: Switching losses, Conduction losses, Fuji simulation, Modulation Index

Date of Submission: 30-09-2021 Date of Acceptance: 13-10-2021

I. INTRODUCTION

The majority of the applications have several loads with different operating voltage ratings, connected to one common supply source. Multilevel converters (MLC) configurations are very much customized for such applications, which develop different voltages for the loads from a common source. NPC, H bridge and Flying capacitor configurations are the basic popular multi-level converter configurations [1]-[3]. Among these converters, NPC converters are regularly employed due to their ease, in their configuration [4]-[6] and control strategies implemented for its operation[7]-[10]. NPC converters are also playing a vital role in HVDC transmission systems and high power drive applications. Figure 1 indicates the NPC converter consisting of twelve IGBT valves with six antiparallel diodes connected to RL load, considered for the analysis in the present work. Sinusoidal pulse width modulation is implemented for triggering the IGBT valve. Clamping diodes will support limiting the power stress across the converter valve. The increase in the converter valves number will lead to the output as close as possible to a pure sinusoidal waveform, by increasing the output levels. This increase in converter elements will lead to losses [11]-[15]. The precise analysis method presented in this paper will help in selecting the appropriate operating mode which will results in almost equal output without extending for higher-level configuration of the converter. This quantitative analysis help in a thorough understanding of NPC converter operation which is a prerequisite to deciding the effective operating mode for NPC converter for a given application. To implement this method the Three-level NPC converter, initially simulated in the MATLAB Simulation tool and then Fiji IGBT simulator.

The algorithm for implementation of the proposed method is

- Step-1: Implement sinusoidal pulse width modulation on three phase three-level NPC converter.
- Step-2: Evaluate the output voltage and current, and Total Harmonic Distortion (THD) of the converter.
- Step-3: Evaluate switching losses and conduction losses by Fuji IGBT simulator.
- Step-4: Validate the converter performance with the analytical method.
- Step-5: Analyze NPC converter operation as a function of Modulation Index.

- Step-6: Analyze NPC converter operation as a function of switching frequency.
- Step-7: Efficiency calculation and optimal operating condition identification.

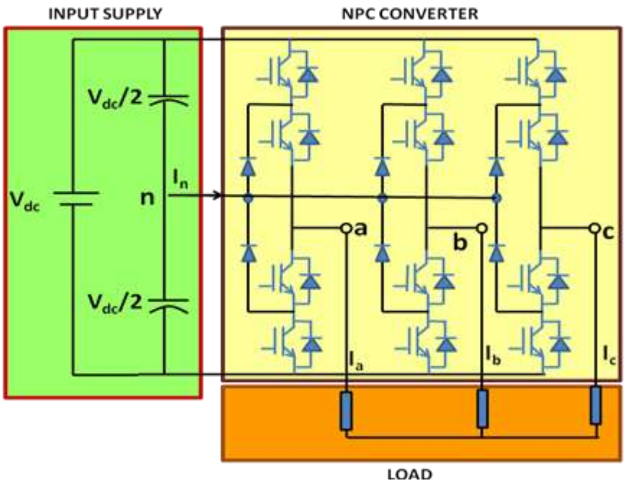

Figure 1. Block diagram of three phase three-level Neutral Point Clamped converter

II. MATLAB SIMULATION OF NPC CONVERTER OPERATION

Simulation block diagram of 600V NPC converter with, 4500V, 400A IGBT valve developed in MATLAB. Simulink block diagram of 500 kW, 400 kVAR RL load, shown in Figure 2 and input parameters assigned for simulation are tabulated in Table 1. Sinusoidal pulse width modulation with 50Hz reference wave, 5kHz carrier frequency is simulated with NOT operator to generate gating pulses for IGBT valves triggering. The input voltage, current, gating pulses for IGBT valves, output phase, and line voltages, output line current, and THD are obtained by MATLAB simulation. Converter losses are simulated by Fuji IGBT simulation. The efficiency of the converter is derived from the MATLAB and Fuji IGBT simulation results.

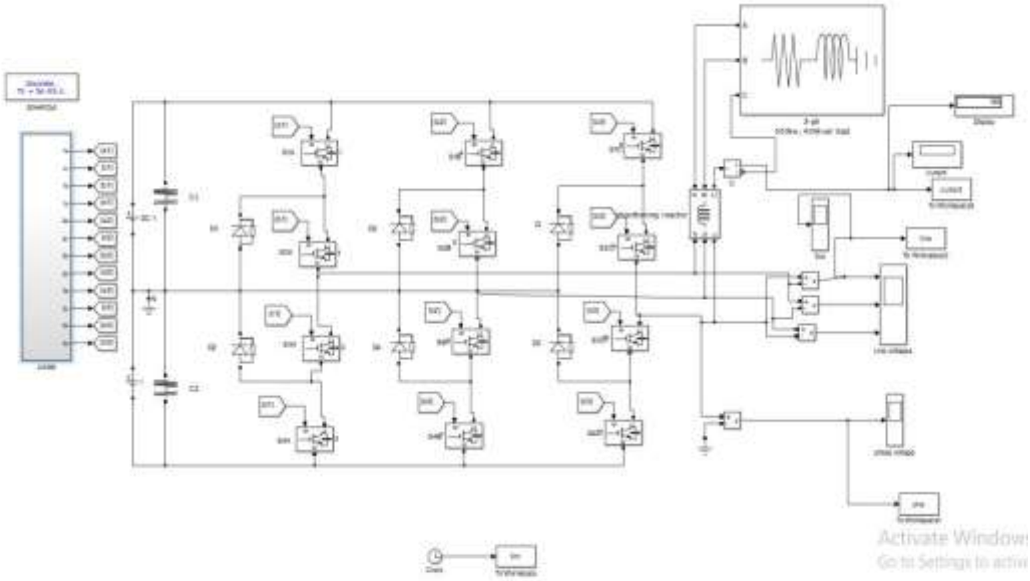

Figure 2. Three-phase three-level NPC converter simulation block diagram

Table 1. Input parameters of three-phase three-level NPC converter for MATLAB Simulation

S.No.	Parameter	Value
1	Input DC voltage (V DC)	600 V
2	Output Current (Io)	150 A
3	PWM technique	Sinusoidal Pulse width modulation
4	Switching Frequency(fsw)	5000 Hz
5	R L load	500kW, 400kVAR

III. VALVE LOSSES EVALUATION BY FUJI IGBT SIMULATION

Fuji IGBT simulation tool supports the simulation of two-level and three-level NPC converters, for different pulse width modulations, chopper circuits. losses estimation, thermal conditions of switching elements, and design aspects of heat sinks [16]. Losses occurring in each element of the converter i.e IGBT and diode during conduction, turn on and turn off modes, and respective temperatures of the elements of the converter are clearly indicates numerically which facilitates a clear analysis of the converters. IGBT valve-based three-level NPC converter, shown in Figure 3, simulated in Fuji software. Table 2 represents, for a particular power factor(PF) and Duty cycle (δ), the converter initial operating conditions of forward voltage (V_{CEO}), collector current (I_c), on-state resistance (Ron), gate resistance (Rg), junction to case thermal resistance (R_{THjc}).

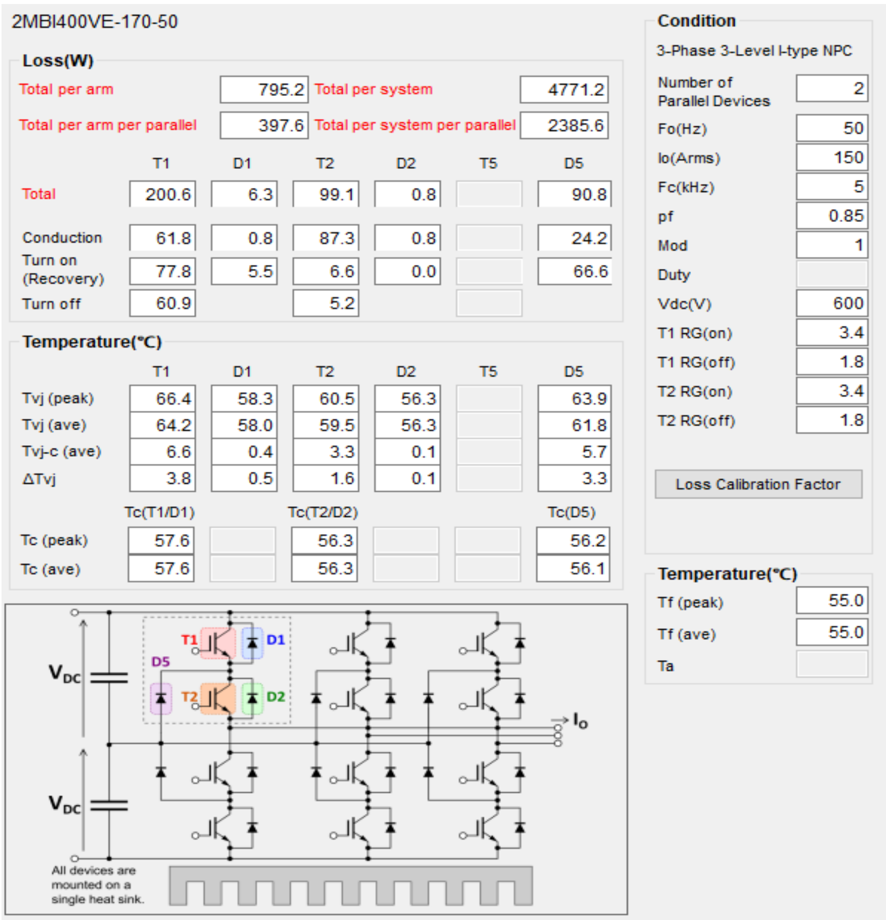

Figure 3. Three phase three-level Neutral Point Clamped converter Fuji simulation diagram

Table 2. Initial operating conditions for Fuji IGBT Simulator

S.No.	Parameter	Value
1.	Voltage	4500V
2.	Current	400A
3.	Forward voltage (V_{CEO})	3.56 V
4.	Collector Current through leg(Ic)	93.8 A
5.	On-state resistance (Ron)	0.0133 Ω
6.	Gate resistance (Rg)	3.4 Ω
7.	Thermal resistance (R_{THjc})	0.052°C/w
8.	Duty cycle (δ)	0.6
9.	Power factor (PF)	0.85

Switching and conduction losses are estimated for each IGBTMBM200H45E2-H, 4500V/400A, IGBT valve for 3 kHz, 5kHz, and 9 kHz switching frequency of operation of the converter. Obtained losses are validated with analytical method values.

IV. ANALYTICAL CONVERTER LOSSES EVALUATION

IGBT valve conduction losses, turn-on losses, turn-off losses, diode on-state losses, and reverse recovery losses are the total losses that occur in the valve. Average losses, for one switching cycle, are calculated. Valve conduction losses vary as a function of the collector to the emitter voltage drop (VCE), collector current (Ic), and duty cycle (δ). Switching power losses occur due to turn-on and turn-off transitions. Switching power losses bank on DC bus voltage (+VCC), collector current (IC), gate resistance (Rg), and switching frequency (fSW). Total losses of the converter are the summation of conduction losses and switching losses, obtained from equations 1 to 4. Based on each valve losses, no of parallel paths of the converter arms total converter losses evaluated and tabulated in Table 3.

$$P_T = P_C + P_{SW} \tag{1}$$

$$P_C = I_C \times V_{CE} \times \delta \tag{2}$$

$$V_{CE} = V_{T0} - R_{CE} I_C \tag{3}$$

$$I_c = \frac{-V_{CEO} + \sqrt{V_{CEO}^2 + 4R_{CEO}\left(\frac{T_{j\max} - T_c}{R_{THjc}}\right)}}{2R_{CEO}} \tag{4}$$

V. RESULTS

Turn on losses, conduction losses, and turnoff losses of the converter for 3kHz, 5kHz, and 9 kHz for 0.8, 0.9, and 1 modulation indices are evaluated analytically compared with that of simulated losses, tabulated in Table 3. Simulation and analytical values are tallying with a minimum deviation of 0.2 units. This error is due to tracing the values manually from the switching characteristic of the IGBT where as simulation values are based on lookup tables data. Converter losses by Fuji simulation are shown from Figure 5 to Figure 13.

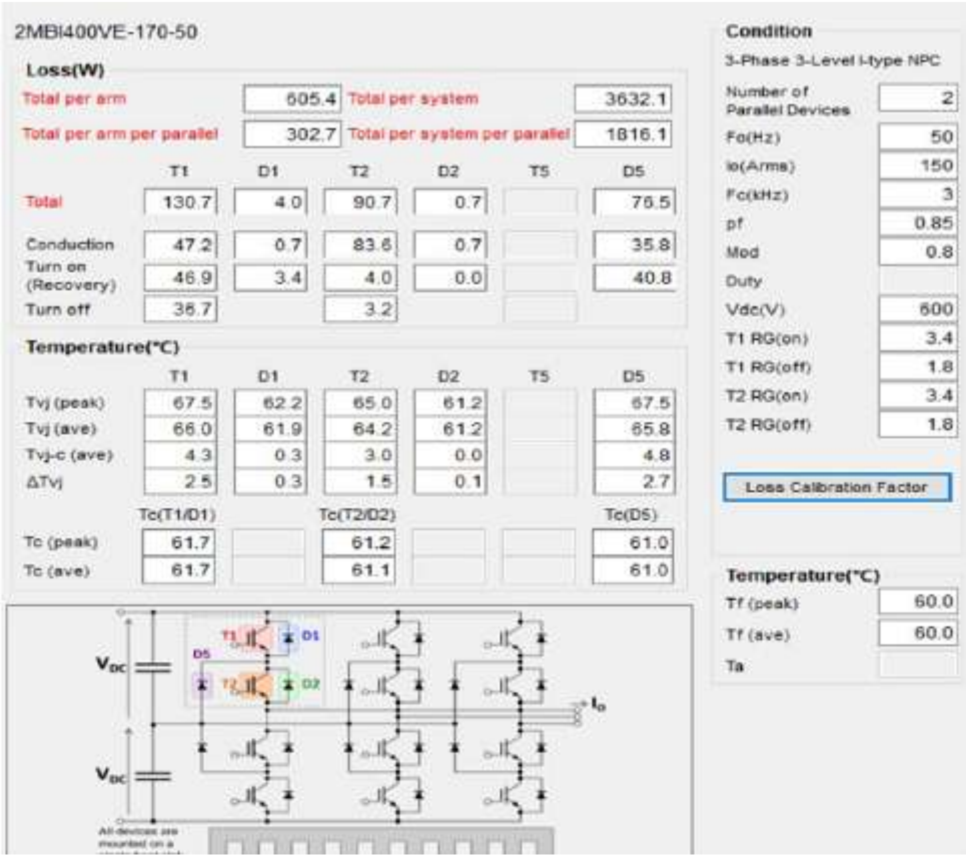

Figure 4: Three phase NPC inverter average losses for 3khz and M.I-0.8

Table 3. Fuji simulation and Analytical converter losses

Three-level NPC converter	Modulation Index (MI)	Fuji simulation				Analytical losses			
		Conduction Losses (kW)	Switching Losses (kW)		Total losses (kW) (system / parallel)	Conduction losses (kW)	Switching losses (kW)		Total losses (kW)
			Turn on (/arm/ parallel)	Turn off (/arm/ parallel)			Turn on	Turn off	
3kHZ	0.8	0.16	0.09	0.039	1.81	0.14	0.987	0.54	1.68
	0.9	0.16	0.094	0.03	1.81				
	1	0.16	0.09	0.04	1.81				
5kHZ	0.8	0.16	0.15	0.06	2.36	0.14	1.64	0.91	2.70
	0.9	0.16	0.15	0.06	2.36				
	1	0.16	0.15	0.06	2.36				
9kHZ	0.8	0.16	0.29	0.12	3.50	0.16	2.96	0.64	3.74
	0.9	0.16	0.29	0.12	3.50				
	1	0.16	0.29	0.12	3.50				

Figure 5 to Figure 13 indicate the instantaneous losses occurring in each IGBT valve and each diode elements. 168.00 W conduction losses (summation of 47.20 W, 0.70 W, 83.60W, 0.70W, 35.80W is 168.00W), 95.10 W turn on losses (summation of 46.90 W, 3.40 W, 4.00 W,40.80 W is 95.10 W) and 39.90 W turn off losses are (summation of 36.70W, 3.20W is 39.90W) and 302.70 W total losses (summation of 168.00 W, 95.10 W, 39.90 W) per arm per parallel, for converter are obtained by simulation of IGBT valve at 3 kHz and 0.8 MI. The complete losses for total system are (302.70x6=1818.00) 1.81 kW. Average losses of IGBT valve at 3kHz , 0.8 MI are (summation of 47.20W, 46.90W, 36.70W is 130.7W) 137 W shown in Figure 4. The instantaneous peak value of IGBT losses are 490 W as shown in Figure 5.

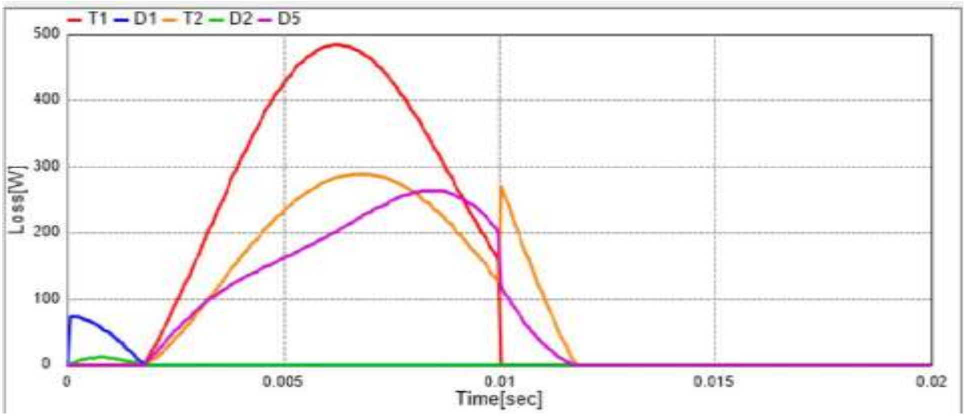

Figure 5: NPC inverter switching elements instantaneous losses for 3khz and M.I-0.8

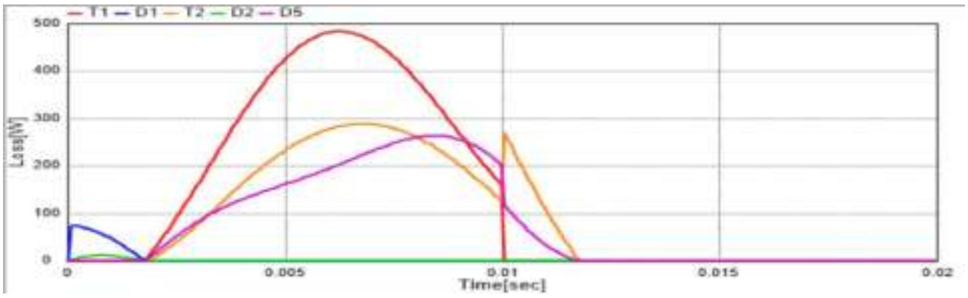

Figure 6: NPC inverter switching elements instantaneous losses for 3khz and M.I-0.9

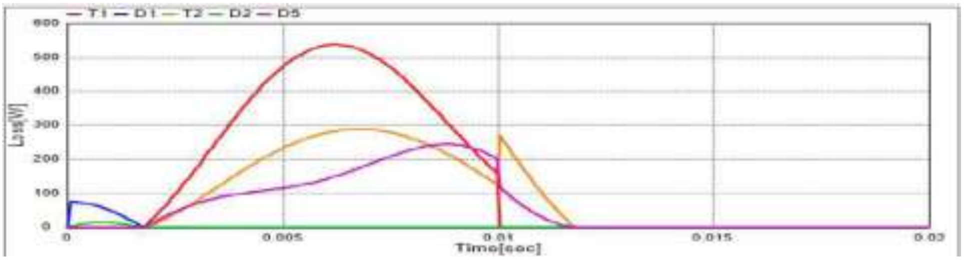

Figure 7: NPC inverter switching elements instantaneous losses for 3khz and M.I-1

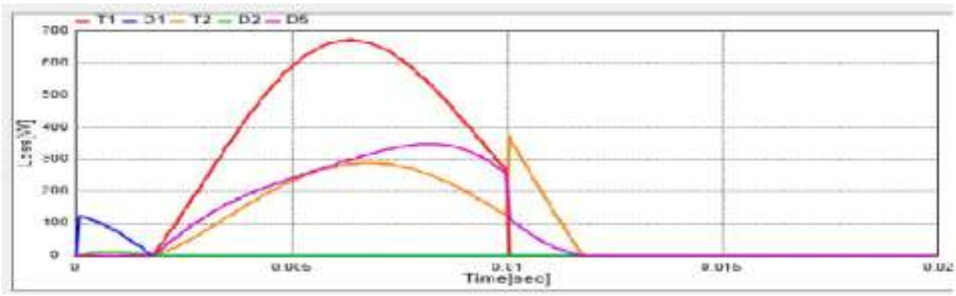

Figure 8: NPC inverter switching elements instantaneous losses for 5khz and M.I-0.8

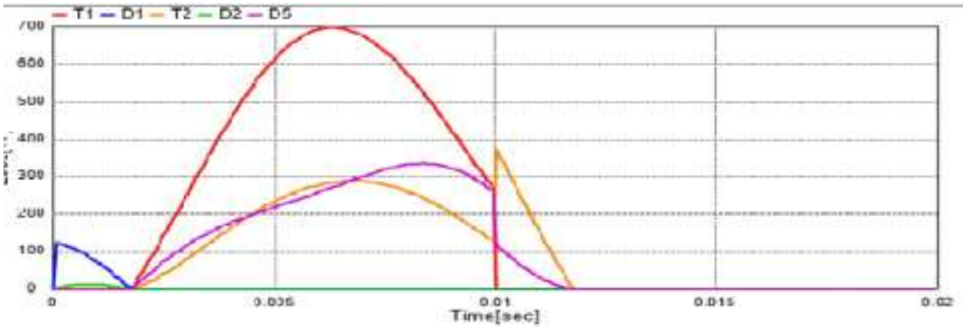

Figure 9: NPC inverter switching elements instantaneous losses for 5khz and M.I-0.9

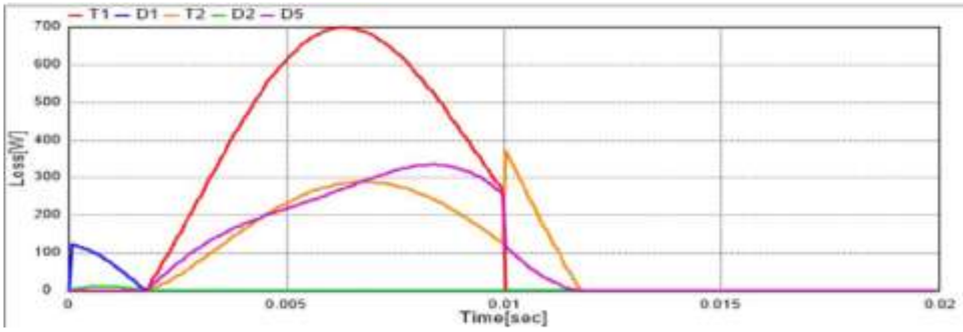

Figure 10: NPC inverter switching elements instantaneous losses for 5khz and M.I-1

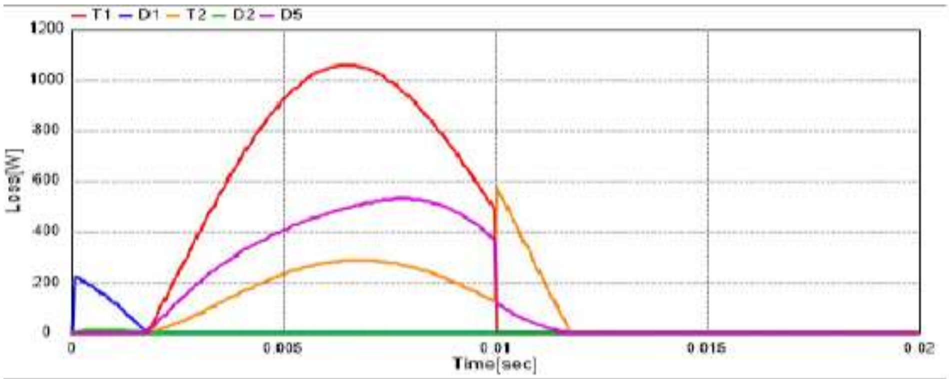

Figure 11: NPC inverter switching elements instantaneous losses for 9khz and M.I-0.8

Figure 12: NPC inverter switching elements instantaneous losses for 9khz and M.I-0.9

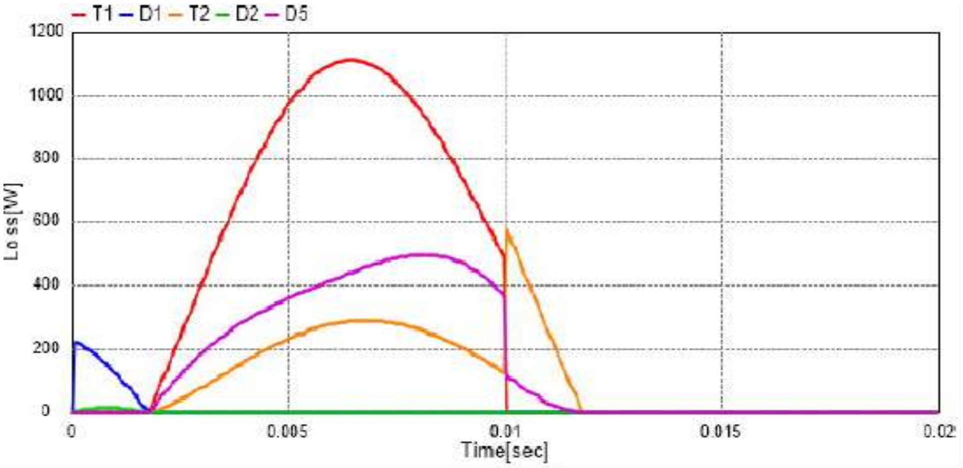

Figure 13: NPC inverter switching elements instantaneous losses for 9kHz and M.I-1

Variation of converter efficiency as a function of modulation index is examined, relating to switching frequencies and tabulated in Table 4. Resulting current and voltage THD are shown in Figure 14 to Figure 19. This analysis will help in selecting the proper operating condition for a specific application. Applications, where the quality of the sinusoidal wave is the priority rather than the output, 5kHz switching mode of operation with 1.70 current THD i.e operating mode with better THD and efficiency can be selected. If output delivered to the load is a priority than the quality, in such applications superior efficiency with bit higher THD mode of operation can be selected. Converter operation for 3kHz -0.9 MI and 1 MI, 5kHz -0.9 MI and 1 MI modes resulting in 97% of efficiency with different current THDs. So among these four modes of operation 5kHz – 0.9 MI, 1.7 current THD, which is lesser THD mode of operation can be opted for given application. This methodology will help in customizing the converter operation as per the application requirement.

Table 4. Efficiency and THD variation as a function of switching frequency

Three-level NPC Converter	Modulation index	Output				THD		Total losses (kW)	Efficiency (%)
		V (V)	I (A)	P.F	P(kW)	V	I	P_T	
3kHZ	0.8	603.50	123.20	0.9	66.91	28.50	3.55	1.81	97
	0.9	603.40	146.00	0.9	79.28	31.71	2.22	1.81	97
	1	603.40	148.60	0.9	80.69	35.50	2.48	1.81	97
5kHZ	0.8	603.50	117.40	0.9	63.76	28.35	3.26	2.36	96
	0.9	603.30	147.50	0.9	80.08	35.10	1.70	2.36	97
	1	603.30	153.70	0.9	83.45	35.11	2.06	2.36	97
9kHZ	0.8	603.50	119.20	0.9	64.74	28.36	3.51	3.50	94
	0.9	603.40	148.00	0.9	80.37	31.48	2.30	3.50	95
	1	603.30	152.70	0.9	82.91	35.33	2.61	3.50	95

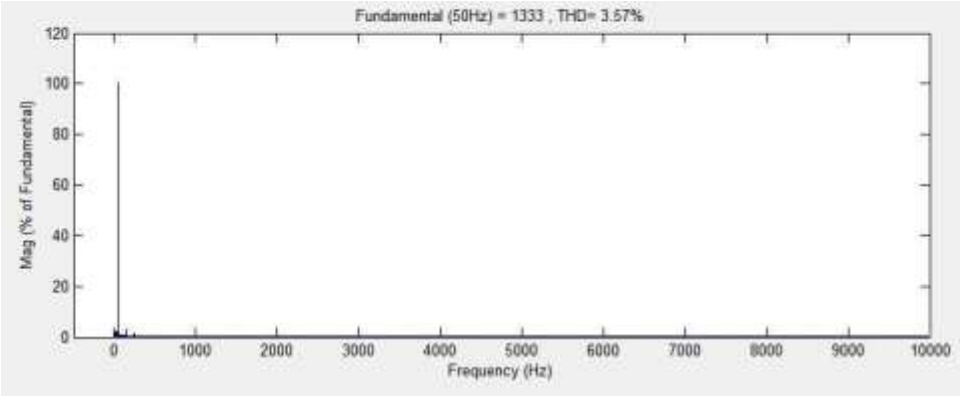

Figure 14: THD analysis for line current of NPC inverter for 3KHz and MI - 0.8

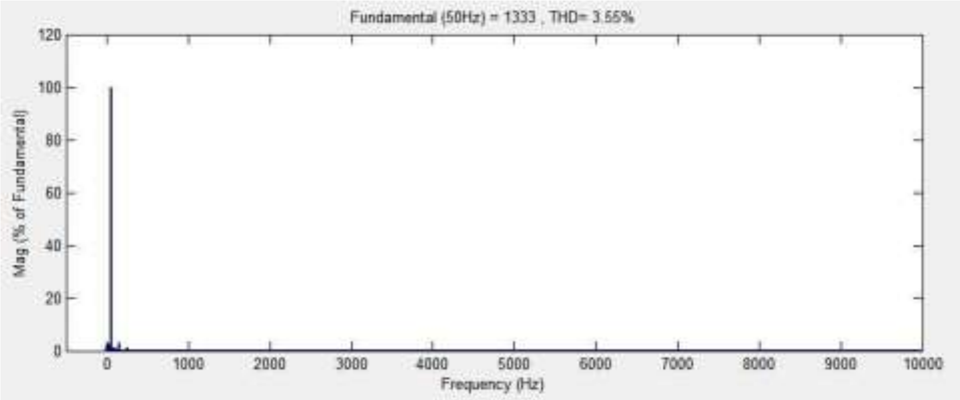

Figure 15: THD analysis for line current of NPC inverter for 5KHz and MI-0.8

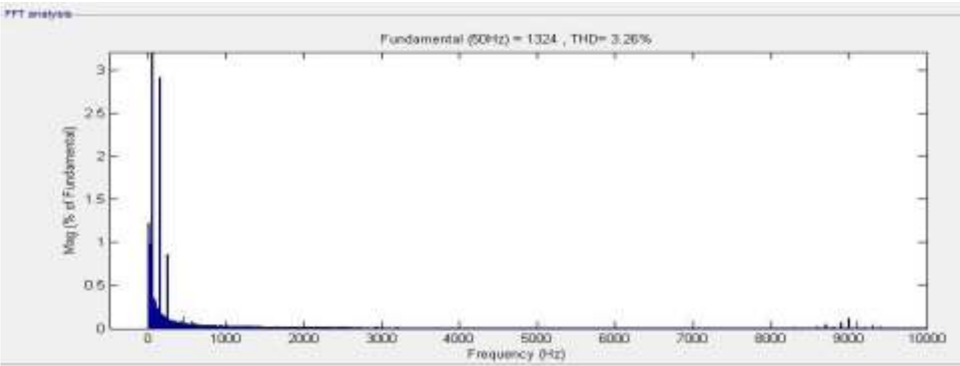

Figure 16: THD analysis for line current of NPC inverter, for 9KHz and MI-0.8

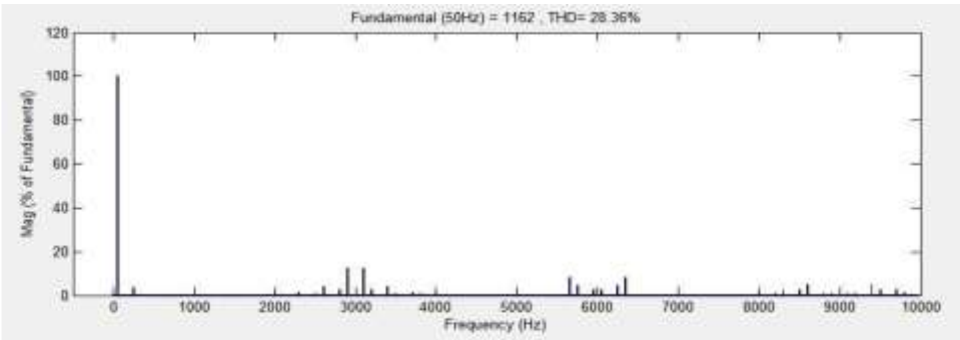

Figure 17: THD analysis for line voltage of NPC inverter for 3KHz and MI-0.8

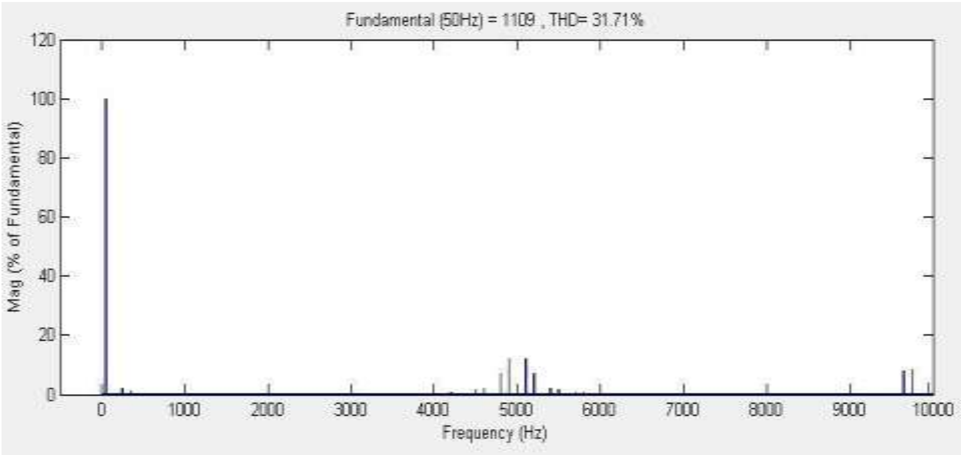

Figure 18: THD analysis for line voltage of NPC inverter for 5KHz and MI-0.9

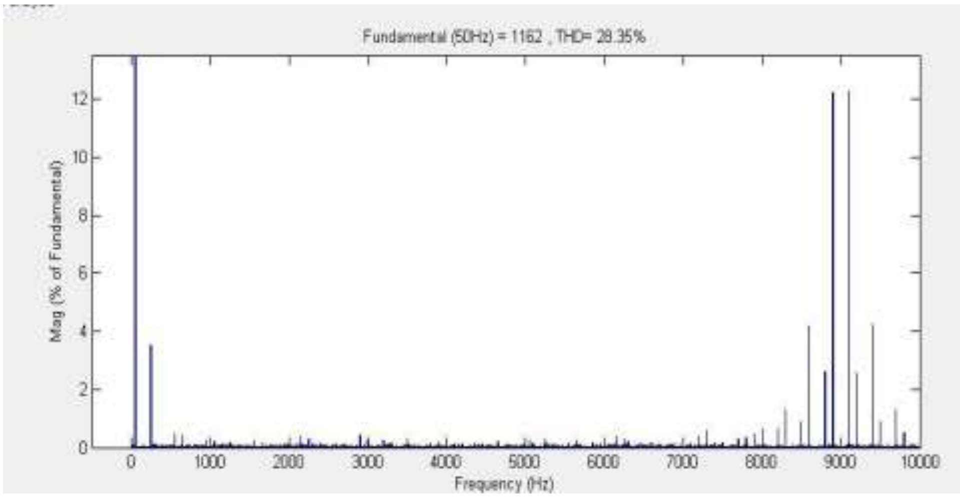

Figure 19: THD analysis for line voltage of NPC inverter for 9KHz and MI-0.8

Figure 20 and Figure 21 present, NPC inverter losses and efficiency variation as a function of switching frequency respectively. 5 kHz operation with 0.9 modulation

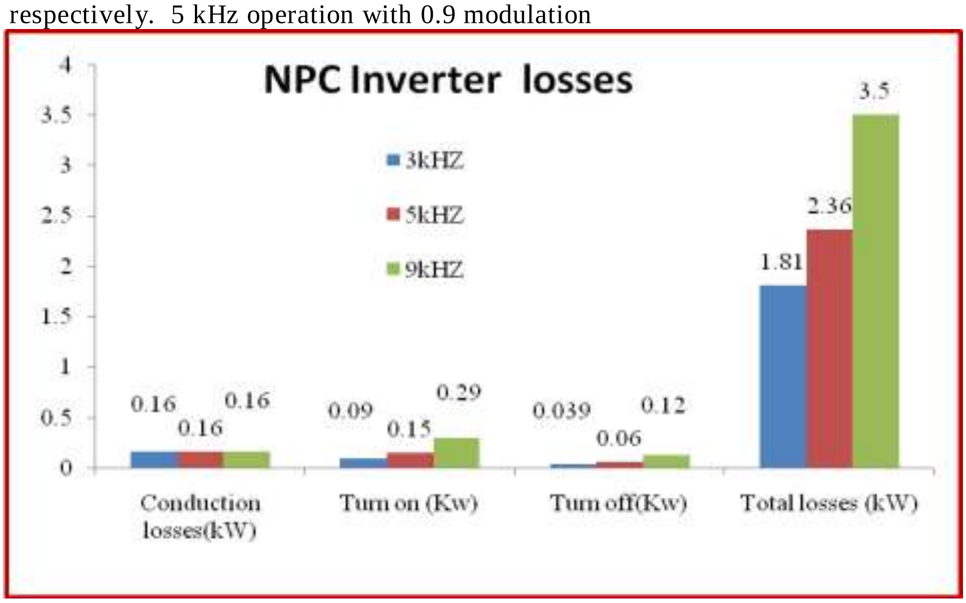

Figure 20: Neutral point converter losses at different switching frequencies

index is resulting in 1.70 current THD and 97% efficiency. This operating mode is superior to the 9 kHz operation which is resulting in 95% efficiency and 2.30 current THD. Each converter valve consisting of two IGBT's along with ant parallel diodes and clamping diode. Conduction, turning on and turning off losses of each element are evaluated and corresponding efficiency is estimated from the obtained losses.

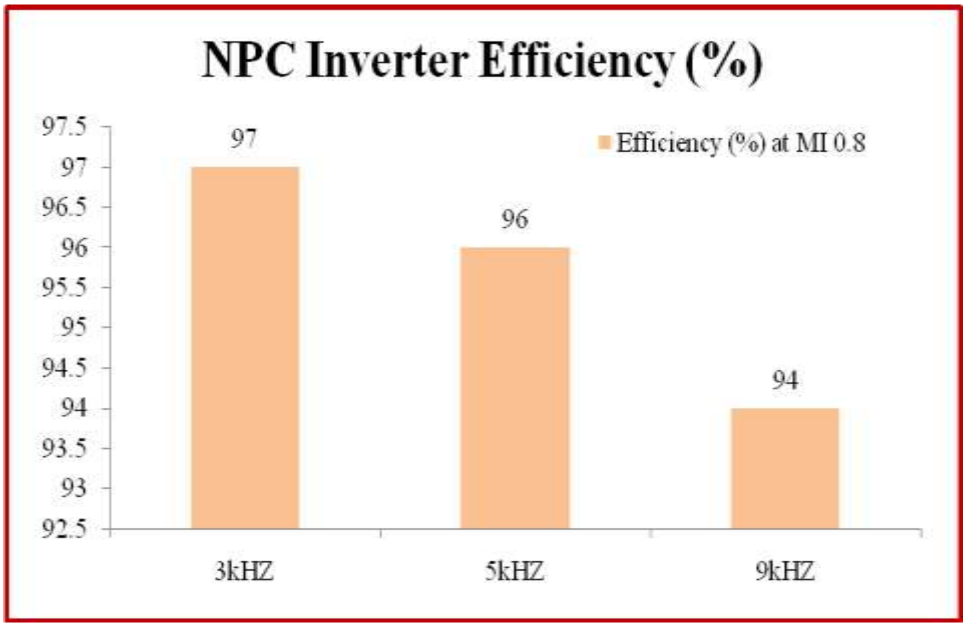

Figure 21: Neutral point converter Efficiency at different switching frequencies

VI. CONCLUSIONS

Higher switching frequency will lead to more losses and lesser efficiency. Opting for higher levels of converters to reduce the THD also leads to more losses due to more switching elements. As the level of converter increases losses, cost, and size of the converter also increase. The precise and meticulous analysis method presented in this paper will help in selecting the appropriate operating modes of the existing converter, which will result in almost equal output, that can be obtained by increasing the converter output levels. This method will help in selecting a relatively higher efficiency, and cost-effective converter mode of operation for a given application.

REFERENCES

[1]. M. Murugesan, R.Pari, R.Sivakumar and S.Sivaranjani " Different Types of Multilevel Inverter Topologies – A Technical Review" International Journal of Advanced Engineering Technology E-ISSN 0976-3945

[2]. Baishali Bhattacharjee, Tilok Boruah and C.Sahu "Comparative Study of Different Types of Multilevel Inverter: With Respect to Output Voltage Waveform" Journal of Energy Research and Environmental Technology (JERET) p-ISSN: 2394-1561; e-ISSN: 2394-157X; Volume 3, Issue 4; October-December, 2016; pp. 240-243

[3]. Ms. Aarya.A, Mrs. Deepa Sankar "Multilevel Inverters-A Comparative Analysis" IOSR Journal of Electrical and Electronics Engineering (IOSR-JEEE) e-ISSN: 2278-1676,p-ISSN: 2320-3331, PP 43-50 www.iosrjournals.org

[4]. J. Rodriguez, S. Bernet, P. K. Steimer, and I. E. Lizama, "A survey on neutral-point-clamped inverters", IEEE Transactions on Industrial Electronics, vol. 57, no. 7, pp. 2219-2230, July 2010.

[5]. Euzeli Cipriano Dos Santos Jr, Edison Roberto Cabral da Silva "Neutral-Point-Clamped Configuration" 26 November 2014.

[6]. https://doi.org/10.1002/9781118886953.ch4

[7]. Vahid Dargahi, Keith A. Corzine, and Arash Khoshkbar Sadigh " A New Three-Level Active Neutral-Point-Clamped (A-NPC) Multilevel Converter Topology" IECON 2019 - 45th Annual Conference of the IEEE Industrial Electronics Society, 09 December 2019, 10.1109/IECON.2019.8927513

[8]. Thilo Janssen, Hariharan Krishnaswami "Voltage and current control of a multi-port NPC inverter configuration for a grid-connected photovoltaic system" June 2016.

[9]. DOI:10.1109/COMPEL.2016.7556699 Conference: 2016 IEEE 17th Workshop on Control and Modeling for Power Electronics (COMPEL)
[10]. Jun-Hyung Jung, Hyun-Keun Ku, Won-Sang I'm and Jang-Mok Kim "A Carrier-Based PWM Control Strategy for Three-Level NPC Inverter Based on Bootstrap Gate Drive Circuit" IEEE Transactions on Power Electronics, 22 July 2019, Volume: 35, Issue: 3, March 2020.
[11]. DOI: 10.1109/TPEL.2019.2930088
[12]. Patricio Gaisse, Javier Muñoz, Ariel Villalón, and Rodrigo Aliaga "Improved Predictive Control for an Asymmetric Multilevel Converter for Photovoltaic Energy" MPDI, Sustainability,1 August 2020.
[13]. J.S.Artal-Sevil, J.M.Lujano-Rojas, C.Bernal-Ruiz, I.Sanz Gorrachategui "Analysis of Power Losses in a Three-Phase Inverter 3L-NPC Comparison with different PWM Modulation Techniques" 978-1-5386-0928-6/18/$31.00@2018IEEE
[14]. A.Mirizadeh, F.A.Baroogh, M.Gheydi, H.Zarrabi and P.Farhadi "Evaluation of conduction and switching losses in cascaded multilevel inverters" International symposium on Advanced Topics in Electrical Engineering (ATEE17), IEEE explore digital library. March 2017
[15]. L.Clotea, A.Forcos, C.Marinescu, and M.Georgescu " Power Losses analysis of two-level and three-level neutral clamped inverters for a wind pump storage system".12th International Conference on Optimization of Electrical and Electronic equipment, OPTIM10. IEEExplore Digital Library
[16]. K.Lee, H.Shin, and J.Choi "Comparative analysis of power losses for 3 levels NPC and T-type inverter modules". IEEE international Telecommunications energy conference (INTELEC). October 2015
[17]. H.Shin, K.Lee, J.Choi, S.Seo, and J.Lee "Power loss comparison with different PWM methods for 3L-T type inverter". International power electronics and Application Conference and Exposition – PEAC 2014.
[18]. A.Babaie, B.Karami and A.Abrishamifar "Improved equations of switching loss and conduction loss in SPWM multilevel inverters" 7th power Electronics and Drive Systems Technologies conference-PEDSTC 2016. IEEE explore Digital Library 2016.
[19]. Fuji Electronics IGBT Module datasheet http://www.fujielectronic.com